

## Evaluation of Various Models Simulate Train Network of LES Created a Shock Wave in a Long Channel

Kazem Kalantari<sup>1\*</sup> and Reza Soleimanpour<sup>2</sup>

1,2-MSc of Mechanical Engineering, Kish International Branch, Islamic Azad University, Kish Island, Iran

**Abstract.** In the present study, the behavior and structure of shock train in a long duct are investigated numerically. In this context, the various subgrid scales of Large eddy simulation model are used to evaluate the ability of those to predict the shock structure. afterward the results are compared with the experimental data of Weiss et al. after ensuring the accuracy of the numerical method, the effects of applying passive and active shock control such as bump and cavity as a passive methods as well as blowing and suction as the active method on the flow behavior are investigated.

**Keywords:** shock wave train, Eddy Simulation large, active and passive flow control

### 1 Background

In the recent years have been conducted various studies on the behavior of the shock wave train from the standpoint of numerical and experimental perspectives. Hatayv studied the phenomenon using impulse wave train Harten-Type second According to two and three-dimensional Navier-Stokes equations numerically And showed that Details can be obtained experimental results obtained using this method.

Gaven and colleagues [2] examined the shock wave series for a nozzle system with both numerical and laboratory bottleneck. They demonstrated experimentally, the dependence of the stationary inlet pressure and flow rate of crime with respect to the structure and position of the system's series of shock waves.

By Grvnza and Oliver [3] investigated experimentally produce shock waves in a small-angle nozzle. They were measured and analyzed using a hot wire, normal Reynolds stress in a series of shock waves. Their results show that by increasing the Mach number, observed two different modes of agitation and the spatial distribution.

Morgan and colleagues [12] examined model simulations of turbulent vortices large vertical shock wave train at a constant level isolator using high-precision equations to predict the behavior of shock waves.

They achieved In comparison Compare with experimental data as closely, the first normal shock wave, The overall structure of the wave field and its interaction with the boundary layer They also predicted using the simulation of physical phenomena such as a lack of reverse flow and development of the secondary layer shear.

## 2 Geometry and boundary conditions

Figure (1) shows the duct geometry is studied in this paper. This is consists of a part converging channel with a length of 50 mm and an angle of 10 degrees, a length of 600 mm and the diverging to a bottleneck in the coordinates (0,0,0) with a height of 6 mm with 5/1 degree angle output.

The existing divergent Three fractures with angles 5/1 and 3 /. Degree at 25 and 160 mm from the throat. In addition, there is a third fracture height are 160 mm to 8 mm. This geometry is defined according to the article Weiss and his colleagues is exactly the same size and model.

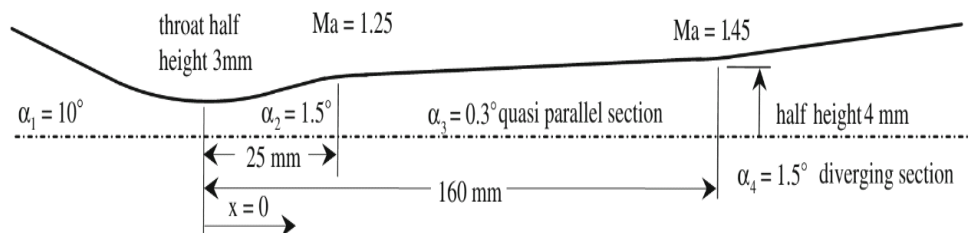


**Figure. 1.** Schema through convergent and divergent reviewed

The simulation should be defined in order to check the proper boundary conditions.

Table (1) shows the input and output is used to simulate the experimental data. It is observed that the flow duct is at 27/89 while the wall temperature is constant. According to the article, Weiss and colleagues [3] to satisfy the speed 27/89, In the present work, provided input to the input pressure is

defined according to whether the static pressure boundary condition and the rest as input, according to the satisfy Ayzentrophic of speed.

It should be noted that at least one of the two static pressure and inertia must be calculated and applied to another according to the article, Weiss and colleagues at work stagnation pressure is equal to 8.4 times. The output pressure is 3.3 bar, as shown in Table 1 is applied to the output condition. For wall temperature of 300 Kelvin and no-slip condition is considered to be fixed during the calculation.

**Table. 1.** The boundary conditions applied in accordance with the data of Weiss and et al [3]

	$P_{total}$ (kPa)	$P_{static}$ (kPa)	T (K)	V (m.s <sup>-1</sup> )
Inlet	490	-	298	89.27
Outlet	-	325	-	-

### 3 Independent review of the results of the computational grid

Is used to evaluate the results of the independence of network computing, and networking in the work of 6 cells for analysis and comparison with previous case.

This analysis has been done for the average Mach three parameters, pressure and speed as shown in Figure (2).

Just as is evident is almost constant for all three parameters in grid computing with cell number 9000000 onwards. According to networking with research work on cell number 9000000 computing. Due to the reduced cost of computing as one of the most important factors in numerical simulations and given that the results in terms of accuracy similar to each other.

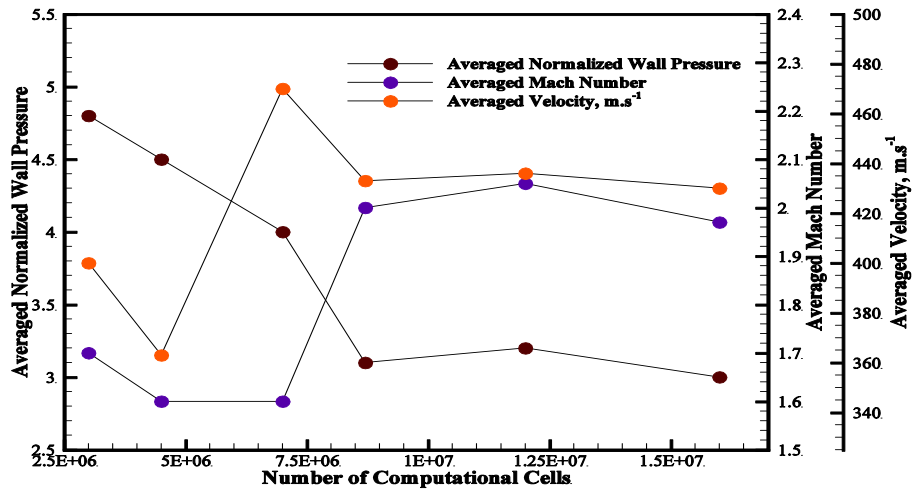


Figure. 2. The results Resolution number of cells

#### 4 Validation of Results

In order to validate the results of the work in This sector to determine the results of simulations with experimental data Weiss and et al. Figure (3) is which represents the pressure distribution along the channel wall for three different the subnets. Just as is evident errors are relatively tangible results the subnets Asmagvrynsky and WALE models In comparison Compare with the WMLES.

Due to higher precision the subnets WMLES Model In comparison with the other two models can be said that these two the subnets models for higher accuracy with more cells are needed to networking. Because of the sensitivity of the two models in the boundary layer, And in front of the WMLES model , Given that the this ability is capable of RANS models to simulate the use of the boundary layer, requires fewer cells, especially in the area; Thus, according to this model better results subnets, the calculation is based on this model.

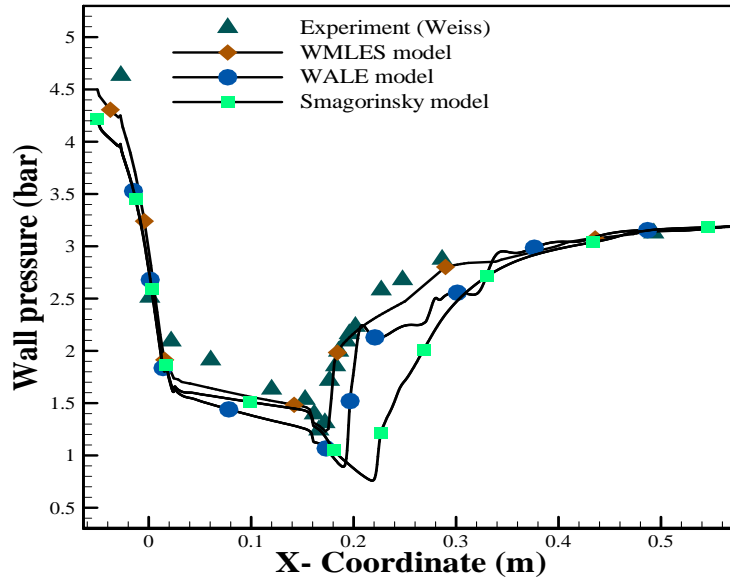


Figure. 3. Comparison of numerical results with experimental data work

### 5 Effects bulge in the wall of the nozzle

This section is addressed to bulge the effects of on the behavior of compressible flow in a convergent - divergent duct with Using subnets WMLES and boundary conditions in Table 1

Projection geometry is obtained using the Hicks-India relationship.

$$f(x) = h_B (\sin(\pi x^{*m}))^t$$

In this regard,  $x^*$ ,  $h_B$ , and  $t$  In this regard, as is the length indicator is dimensionless, using the dimensionless bulge, bump height and the tilt controls parameter , And their values are shown in table (2).

Table. 2. Profile of the bulge

$h_B$	$c_B/l_B$	$t$	$l_B$
0.001c-0.01	0.4-0.85	0.5-3.0	0.25c

Also,  $m = \frac{\ln(0.5)}{\ln\left(\frac{C_B}{l_B}\right)}$  is the asymmetry index between 0 and 1.

Figure (4) (in the left corner bottom) depicts the protrusion schema used. As well as Figure (4) shows wall pressure distribution for 4 different modes with different ratios of  $h$  to  $l$  including 04/0, 06/0 and 08/0 and without control. As well as the figure is drawn pressure connectors

With regard to figure, is evident when you use two and four states, increased pressure fluctuations and also for modes 1 and 3, the shock wave moves towards upstream. Increase the pressure fluctuations Means an increase in energy loss and pressure loss is Increase, so methods (cases 2 and 4) are not sufficient to control the flow behavior Because it reduces the efficiency of their systems. The reason for this phenomenon seems to increase the thickness of the boundary layer flow upstream, as well as a nozzle protruding length is less than the height bottleneck.

It is also clear that the use of Mode 3 with regard to the changes, the pressure drop is less, so the shock wave power is low.

Figure (5), which represents the plate along the  $x$  axis passes through the center of the nozzle, and includes contour Shadvgraf for scenarios 1 and 3. The structure of shock waves reflected well on this picture indicates that increased the distance between the waves when the swell is used for a branch. Thus, the power of the waves in the distance between the branches, that it will be reduced by increasing the power of the waves.

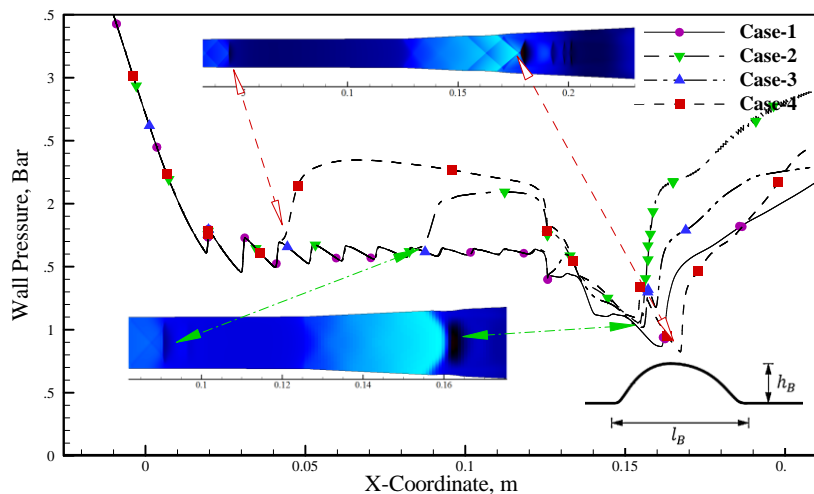
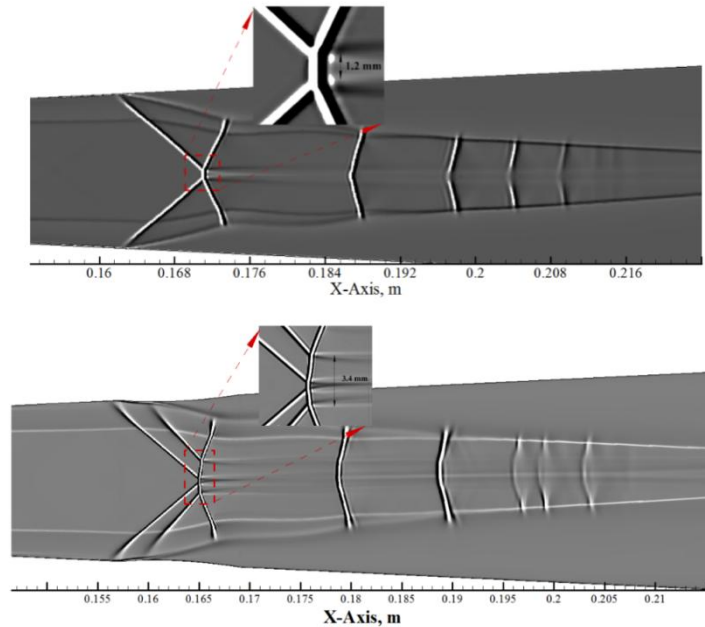


Figure. 4. Distribution of pressure walls with lumps and without that



**Figure. 5.** Contour Shadygraf the normal bumps and Mode 2

## 6 The effects of passive holes

This section focuses on the effects of holes as a passive flow control method. How cavity design was the same as projection design, The only difference is that contrary to bulge. Turn holes are placed at the site of shock wave. Results showed a significant effect on the flow behavior is applied to the cavity.

Figure (6) shows the normalized pressure distribution of the wall. It is known as pitting reduces the pressure drop is, the current loss decreases with increasing hole depth. As well as increased pressure at the top of the cavity is because of the Prandtl -Meyer compression waves in the cavity because of the hogging along the wall.

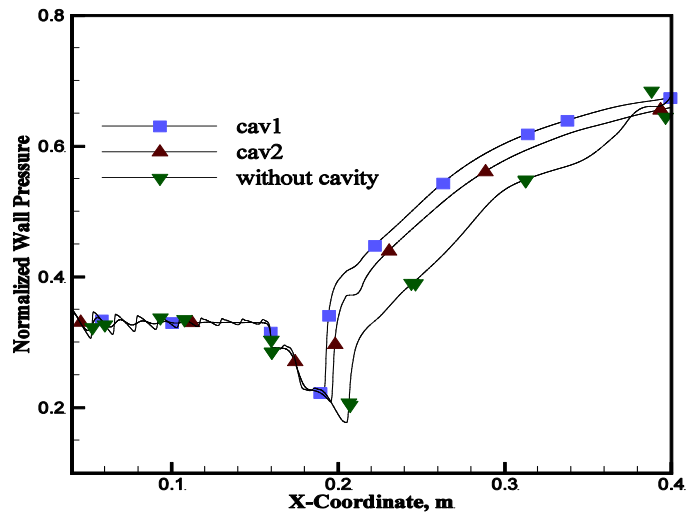


**Figure. 6.** Distribution of pressure normalized for cases with holes and without a cavity wall

The cavity caused a suction pump flow and the downstream flow is disabled and the wave power stroke is reduced. As the Figure (7) is specified, when the cavity is used, the maximum Mach number decreased with increasing hole depth and reduce the shock wave Mach number indicates a reduction in power and therefore energy loss is reduced.

In addition to the bottleneck has moved the location of the shock wave as the hole depth increases because the thickness of the boundary layer downstream will rise further.

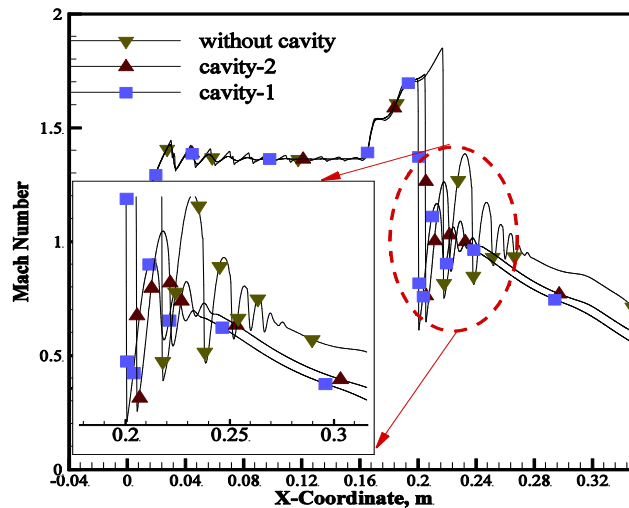


**Figure. 7.** Distribution of Mach number on the center line conduit for cases with The cavity And the without The cavity

Figure (8) shows the distribution is related to  $\frac{u}{a} \frac{\nabla P}{\sqrt{P_x^2 + P_y^2 + P_z^2}}$  would

be appropriate to show the number of waves.

This relationship will be given when  $\sqrt{P_x^2 + P_y^2 + P_z^2} < 0.14P_\infty$  is zero.

This relationship will be very suitable as a way to predict the number of shock waves. Figure (7) shows the distribution of the relationship between the central line of the nozzle.

It is obvious that without holes (unchecked) the number of waves is equal to 6 if the number is low when the cavity shock waves. This phenomenon is due to reduced flow Mach number when there are holes in the duct.

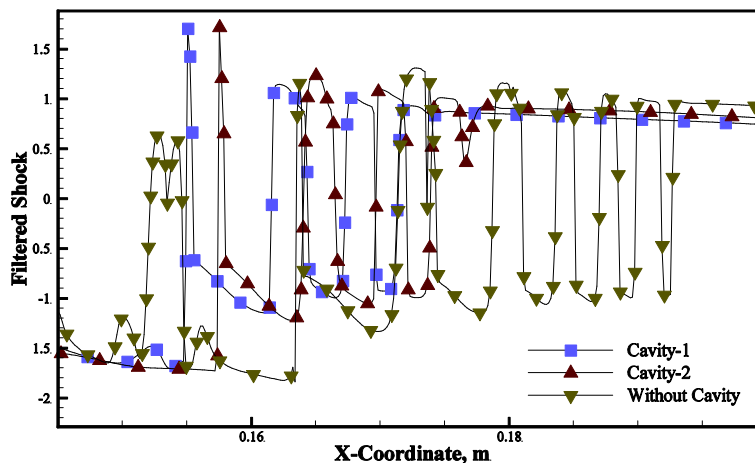


Figure. 8. Distribution function of  $\frac{u}{a} \frac{\nabla P}{\sqrt{P_x^2 + P_y^2 + P_z^2}}$  the central line conduit for cases with

holes and without holes.

## 7 The Effect of Suction

There are several ways to control the boundary layer and separation attempts. One of these methods is to create suction in the flow separation point. This method as a way to control the behavior and structure of the course is accompanied by shock waves. In this section are the effects of suction on how to change the current structure has been studied. Boundary conditions are in accordance with the table (1) The difference is that in the place where the shock wave is embedded in two locations to create suction with crime rates 2.1 and 4.2 kilograms per second. The results show that the flow behavior compared with normal controls, and even more significant changes will increase the suction rate changes. For

suction mode with a crime rate of 2.1 kg per second, the physics is similar to the structure of shock waves. But with increasing rate of flow from the suction nature is out of control. Since reduced the number to less than 5/1 the intraluminal Mach. In view of the contours of the form (4-9), Mach number flow without suction mode and Mode 2, respectively, and approximately 8/1 and is 6/1. So there are situations shock waves extended; However, as shown in the figure, in Mode 3, reached Mach 4.1 flow. There is not a condition of shock waves long gone and the shock wave plug.

Another result of the (9) is achieved:

Using suction, reducing the strength of the shock wave, because Mach reduction From 8/1 to 6/0, From 6/1 to 7/0 And 4/1 to 7/0 respectively is for scenarios 1 to 3.

It can also be noted that the use of suction, pressure loss is reduced because of the shock waves. This is due to a direct effect of the intake to slow down the boundary layer and reduced friction losses. There is also suction to stabilize the laminar boundary layer is therefore reduced boundary layer and it quickly becomes more uniform distribution. Another reason is to reduce the suction power of the shock wave by delaying the transition from laminar to turbulent flow and also delaying the flow separation of the boundary layer. Figure (10) is indicated Shadygraf meters. As it is clear by using suction flow is quite different to the current structure of the distance between the throat and the position of the suction system. As noted above, when using suction crime rate is 2/1 the bifurcate structure. But for Mode 3 does not form this structure, that this good results shown in the figure.

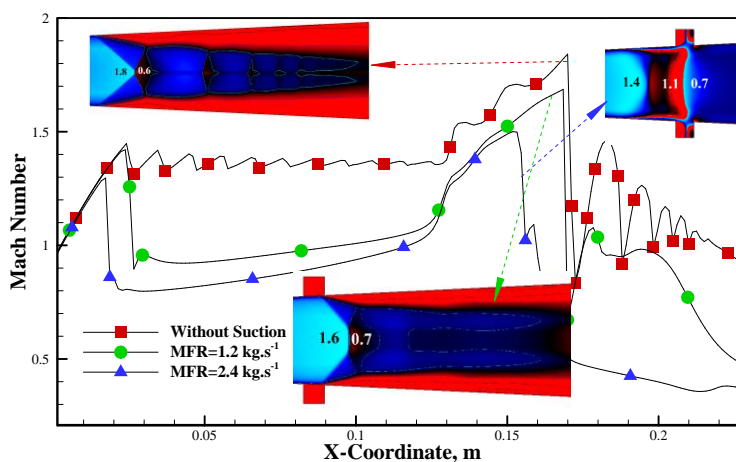


**Figure. 9.** Distribution of Mach number on the center line of the duct

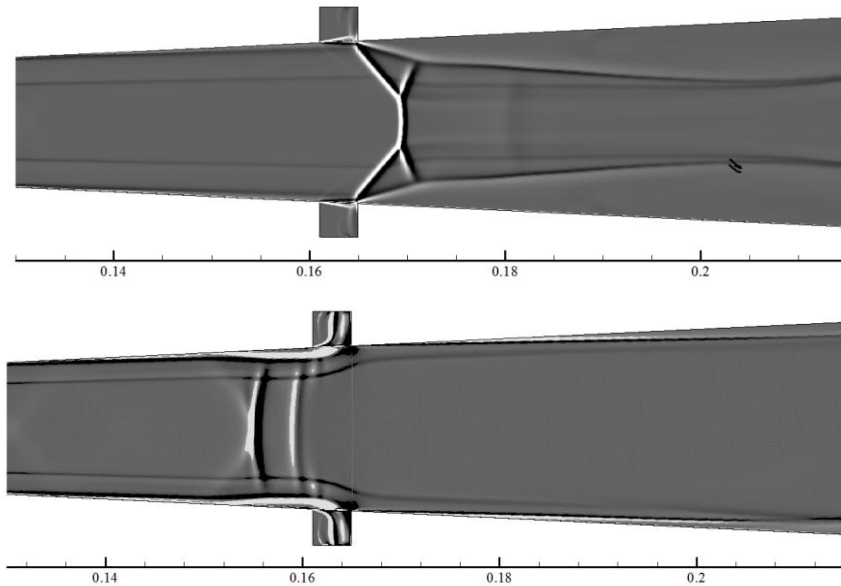


**Figure. 10.** Contour Shdvgraf for modes using suction

## 8 The effects of tail on the flow

As suction pump as an active method is used to control the flow. This section is also intended using tail and its effect on the structure of the shock wave. Studies have been done for of 3 different sample streams. These are three examples of crime rates 5/0, 2/1 and 5/1 kilograms per second. In this regard,.

Figure (11) shows the wall pressure distribution for each of the three modes. The results show clear changes in the structure of waves is using this technology. By increasing the pumping rate, increased by fluctuations in the distribution of pressure and pressure drop. This means that wave power will increase the impact by increasing the pumping rate. Because there is coated wall shear stress decreases.

However, it is observed that the distribution of pressure for different scenarios are almost similar.

Figure (12) shows the contour of the three modes is listed above. As is known, by increasing the pumping rate of the first wave of shock, the branch moves the nozzle throat and the distance between the first and second shock wave will be increased. In addition, with the increasing crime rate pumping, increase the number of shock waves; In other words, fans of the tail thickness reduces momentum And distribution optimizes the velocity profile resulting in the more sustainable the boundary layer.

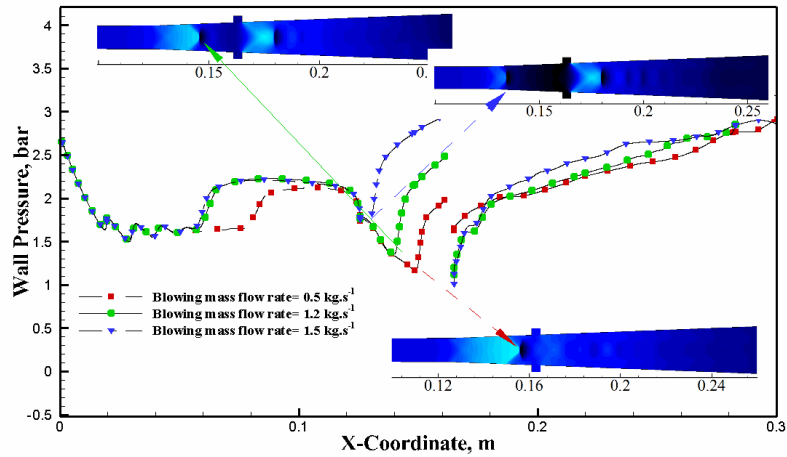


**Figure. 11.** Distribution of pressure walls for different crime rate in the case of tail

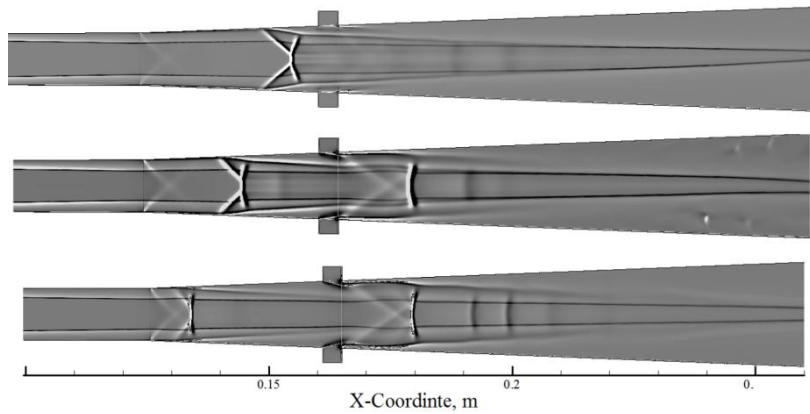


**Figure. 12.** Contour Shadygraf to tail with different crime rate

## 9 Conclusion

In this paper was investigated to evaluate numerical flow behavior in a convergent divergent duct using Fluent software. After validation, the method used was done by comparing the numerical results with experimental data published in this prestigious journal and there was investigated a bulge, holes, and suction pump and overall results were obtained as follows.

1. A WMLES subnet model is a good way to simulate the internal structure of compressible flow.

2. The branch has increased the distance between the waves, while the bulge is used, Thus, the power of the waves in the distance between the branches, which with the increase it, Wave power will be reduced.

3. pitting reduce the pressure drop, which slump flow test decreases with increasing hole depth.

4. Using suction reduced pressure loss due to shock waves.

5. By increasing the pumping rate, fluctuations in the distribution of increased pressure and increased pressure drop.

## REFERENCES

1. Hataue I: Computational study of the shock-wave/boundary-layer interaction in a duct. *Fluid Dyn Res.* 1989, 5(3), 217-234.
2. Gawehn T., Gülhan A., Al-Hasan N.S., Schnerr G.H., Experimental and numerical analysis of the structure of pseudo-shock systems in Laval nozzles with parallel side walls, *Shock Waves*, 2010, 20, 297–306.
3. W. Huang, Z.-g. Wang, M. Pourkashanian, L. Ma, D.B. Ingham, S.-b. Luo, J. Lei, J. Liu, Numerical investigation on the shock wave transition in a three-dimensional scramjet isolator, *Acta Astronautica*, 68 (2011) 1669-1675.
4. Morgan B., Duraisamy K., Lele S.K., Large-Eddy Simulations of a Normal Shock Train in a Constant-Area Isolator, *AIAA Journal*, 2014, 52, 539-558.
5. Weiss, A., Grzona, A., and Olivier, H. "Behavior of shock trains in a diverging duct," *Experiments in Fluids* Vol. 49, No. 2, 2010, pp. 355-365.